

# Flooded Areas Detection Based on LBP from UAV Images

ANDRADA LIVIA SUMALAN, DAN POPESCU, LORETTA ICHIM

Faculty of Automatic Control and Computers

University Politehnica of Bucharest

Bucharest, ROMANIA

a.sumalan@gmail.com, dan\_popescu\_2002@yahoo.com, iloretta@yahoo.com

*Abstract:* - In this paper, a methodology is proposed for the detection of the flooded areas, considering the development of an algorithm based on Local Binary Pattern operator which is extended in order to be applied on Green and Red channels of RGB and H of HSV. The process of image acquisition is realized by a camera incorporated in a fixed-wing UAV. The proposed algorithm is based on the consideration of three classes (flood, grass and buildings) and its purpose is to determinate the adequate class for each tested sub-image extracted from images than contain flooded areas. The process of decision is extended to the three color components and it is realized by computing the distance from the histogram vector of the tested sub-image to the average histogram vectors of the classes determined on each color component. The use of LBP operator and the development of the proposed algorithm on the three color components improve the process of classification of the sub-images to a specific class.

*Key-Words:* - Local Binary Pattern, histogram, flood detection, color channels, image classification, UAV

## 1 Introduction

Floods are the costliest types of natural catastrophes in the world and it accounts for 31% of the economic losses resulting from natural catastrophes.

In order to reduce flood impact on communities and environment, it is necessary to manage the flood risk in a sustainable and coordinated way.

Taking measures, both structural and non-structural, to reduce the likelihood of floods and the impact of floods in a specific location, involve the detection and evaluation of the affected areas.

In [1], the authors present a video surveillance method based on the consideration of the flood overflow as a monitoring object using processing images acquired by a remote cyber surveillance system. This method is proved to have a relatively high robustness in outdoor flood detection and warning applications.

Taking into consideration statistical and fractal characteristics, in [2] the authors propose a method of image classification in UAV monitoring application.

In [3] research, optical imagery is acquired by a mini-UAV to monitor the serious urban waterlogging in Yuyao, China. Texture features derived from gray level co-occurrence matrix are included to increase the distinction of different ground objects. A Random Forest classifier,

consisting of 200 decision trees, is used to extract flooded areas in the spectral-textural feature space.

Another flood monitoring technique using adjustable histogram equalization is proposed in [4]. The proposed technique takes pre-images and post-images and applies different processing steps for generating flood map without user interaction. The resultant flood maps can be used for flood monitoring and detection.

In study [5], two region-based image segmentation methods, Grow Cut and Region Growing (RegGro), are applied to rain scenes. The authors demonstrate that segmentation accuracy depends on fog and rain stains.

As shown in [6], texture characterizes the spatial distribution or repetitive levels of intensity / color of the surfaces of the areas of interest. Methods for extracting features from texture are classified in 4 categories:

- a) structural: use primitives to describe texture elements and to find rules for computing the spatial relationships between elements;
- b) statistics: correlation function, operators on edges, gray level co – occurrence matrix;
- c) analysis on frequency domain;
- d) model-based techniques, like fractals.

Descriptions are the type of distributions of certain characteristics (value, energy, variation) in

the space field or in the field of image frequency (spectral characterization).

The areas affected by natural disasters can be detected by using a fixed-wing UAV which represents a cheap and affordable option. The advantages of fixed-wing UAVs over conventional satellites are represented not only by the low-cost high resolution image acquisition capability but also by the reasonable costs for the capacity of revisiting the same location weekly or daily in some cases.

## 2 Methodology

Local Binary Pattern operator represents an efficient way of analyzing textures and it incorporates both properties of structural and statistical texture analysis methods.

The proposed methodology for the detection of the flooded areas considers the development of an algorithm based on Local Binary Pattern operator.

Local Binary Pattern (LBP) is an operator that provides a high discrimination mechanism for images. The most important feature of the LBP operator is the tolerance to illumination changes and the simplicity of calculation. The LBP logic consists in assigning for each pixel of the image a binary number resulted from the comparison of the iterated pixel and all its neighbors that are determined based on the distance established from the iterated pixel [7].

The definition of the comparison is defined in (1) and it is represented by the difference in value between the iterated pixel  $p_{i,j}$  and a neighbor  $n_k$ .

$$c(p_{i,j}, n_k) = \begin{cases} 1, & V(p_{i,j}) - V(n_k) \geq 0 \\ 0, & V(p_{i,j}) - V(n_k) < 0 \end{cases} \quad (1)$$

The result of the comparison is used to create a binary number starting from left with the value for the first neighbor  $n_1$  and ending with the value for the last neighbor  $n_{nk}$  (2).

$$LBP_{bin} = c(p_{i,j}, n_{nk}) \dots c(p_{i,j}, n_1) \quad (2)$$

After the computation of the binary number, the *LBP* code is calculated as in (3).

$$LBP = \sum_{l=1}^{n_{nk}} LNP_{bin}(l) \cdot 2^{l-1} \quad (3)$$

Consequently, the methodology established the value 1 for the distance from the iterated pixel and

all its neighbors, meaning that the number of neighbors that must be checked is equal to 8 [8].

In other words, for each pixel of the tested image the differences between its value and the values of the 8 neighbors are computed, by starting with the pixel from the top left-corner and continuing with all the other neighbors clockwise. Based on these differences, an eight-digit binary number is assigned to each pixel, this number being the determined binary *LBP* code on which it is applied a conversion to base 10 [9]. Figure 1 presents a graphical example of application of the *LBP* operator.

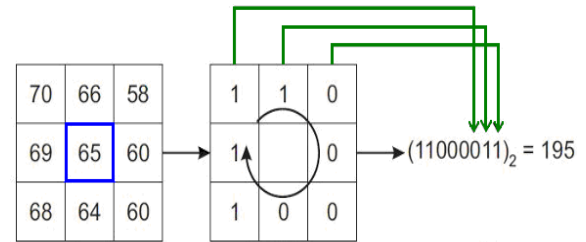


Fig.1. Computing *LBP* code example.

After the computation of the *LBP* codes, the histogram of the image being the distribution of the *LBP* codes is generated and also the vector that contains the number of *LBP* codes that have a value within a specific domain is retained [10]. The purpose of this vector is to differentiate images based on the number of *LBP* codes from different value domains.

In this paper, *LBP* is extended in order to be applied on different channels of RGB and HSV color spaces. The *LBP* operator is applied to Red and Green channels from RGB and H component of HSV. The Blue channel from RGB is not selected because this color is present in very small quantities in the flood images and also a grayscale transformation would only darken the image. Regarding HSV color space, the S component is not applicable since the levels of lightness are medium to high in the flooded regions and by extracting this component, these regions would become darker. The V component is also not suitable since it is very sensitive to variation in the illumination. On the other hand, the H component is not affected by these variations [11].

Since the purpose is to recognize different classes in the images of flooded areas, the first part of the proposed methodology is defined as a learning phase in which the classes are built by applying the *LBP* operator on suggestive sub-images of dimensions 256×256 extracted from images of dimensions 4000×6000. In other cases,

the dimensions of the sub-images can be established to  $128 \times 128$ ,  $64 \times 64$  etc.

The defined classes are the sub-images with flood, the sub-images with grass and the sub-images with buildings.

After this part, the learning phase is ended and each class is represented by a vector obtained through averaging the vectors of the sub-images used in the learning phase.

The second part of the proposed methodology is represented by the assignment of the tested sub-image to one of the three classes by comparing the histogram vectors of the sub-image with the vectors of the classes generated in the learning phase. The assignment of the sub-image to one of the three classes is realized by calculating the Euclidean distance between these vectors.

The Euclidean distance between the histogram vector of the tested sub-image  $V_T$  and the histogram vectors of the classes  $V_C$  is computed as it follows:

$$d(V_T, V_C) = \begin{bmatrix} \sqrt{\sum_{i=1}^n [V_T(i) - V_{C\_F}(i)]^2} \\ \sqrt{\sum_{i=1}^n [V_T(i) - V_{C\_G}(i)]^2} \\ \sqrt{\sum_{i=1}^n [V_T(i) - V_{C\_B}(i)]^2} \end{bmatrix} \quad (4)$$

where  $V_{C\_F}$  is the average histogram vector for the flood class,  $V_{C\_G}$  is the average histogram vector for the grass class,  $V_{C\_B}$  is the average histogram vector for the buildings class and  $n$  is the number of elements of the histogram vectors [12].

The vector  $d(V_T, V_C)$  has three elements that represents the calculated distance between the histogram vector of the tested sub-image and the average histogram vectors of the three classes for each color component.

The tested sub-image is framed in the class that is correlated with the smallest value found in the elements of vector  $d(V_T, V_C)$ .

This step of affiliation of the tested sub-image to a specific class is repeated for each one of the three color components of the tested sub-image.

Finally, the process of decision is realized based on the condition that if the tested sub-image is in correspondence with a certain class for at least two color components, then this sub-image belongs to that class (flood, grass or buildings).

### 3 Algorithm

The design of the algorithm for the proposed methodology is presented in figure 2. As it can be observed, the algorithm is divided in 2 parts:

- Learning phase in which from various flood images, representative sub-images of the three classes are extracted and based on this selection and using the LBP operator, the average histogram vector for each type of class are calculated [13].

- Testing phase in which any sub-image of a flood image is loaded; using LBP operator, the histogram vector is calculated and the decision of affiliation of the loaded sub-image to one of the three defined classes is made by evaluating the distance between its histogram vector and the average histogram vectors of the three classes.

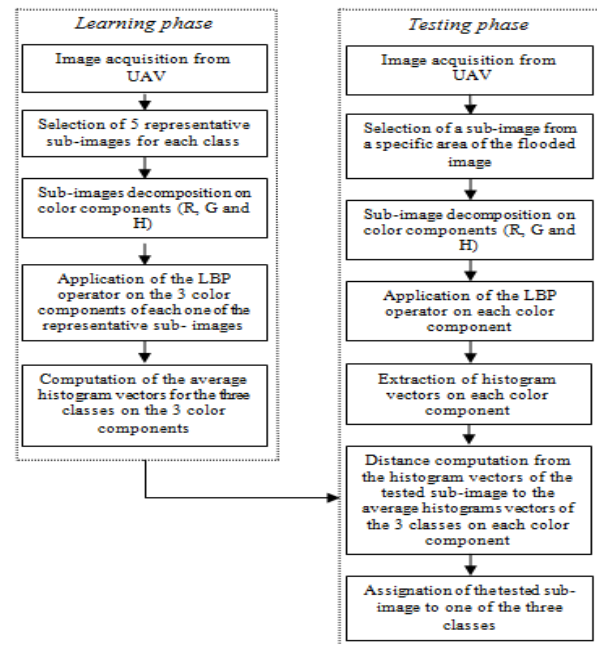


Fig.2. Major steps of the proposed method.

### 4 Experimental Results and Discussions

In this paper, a fixed-wing UAV system was used. HIRBUS [14] is a compact system with double purposes, used both in military and civilian applications. Its structure has the following elements:

- HIRBUS unmanned aircraft;
- Ground Control Station (GSC);
- Data link;
- Launcher.

Its main features are:

- Retractable gyro-stabilized payload;

- b) “Camera follow” navigation;
- c) High resolution imagery;
- d) GIS support;
- e) automatic navigation;
- f) operation in various types of environment;
- g) extended operational range using multiple Ground Data Terminals;
- h) mission planning software application.

The images and sub-images acquired by the HIRBUS system and selected for the determination of the average histogram vectors for the classes are shown in figure 3 in which for each flood image the representative sub-image is indicated.

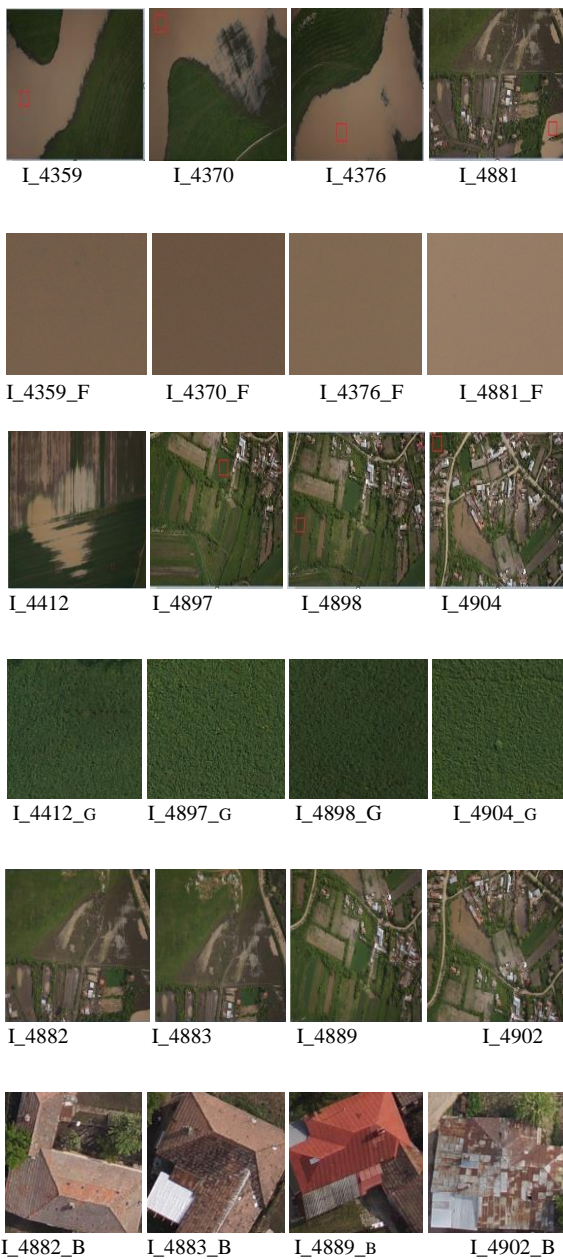
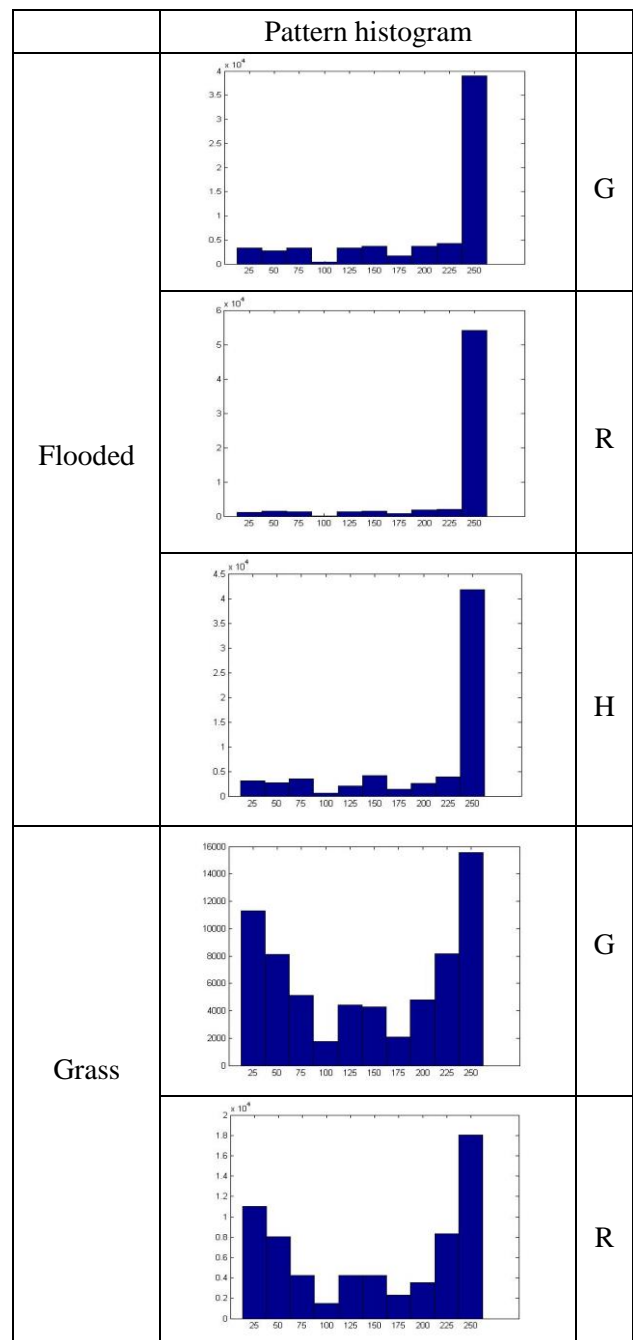


Fig.3. Images and sub-images selected for computing the histogram vectors for the 3 classes.

The average histograms for each class are presented in figure 4 divided in each chosen component. As it can be observed, the histograms for the flood class in all components highlights the fact that the number of LBP codes with values higher than 200 is much bigger than the number of LBP codes with the values lower than 200. On the other hand, the histograms of grass and buildings classes contain a bigger number of LBP codes with values lower than 200. Following this, there is a significant difference between the obtained flood class and the obtained grass and buildings classes by just comparing the histograms.



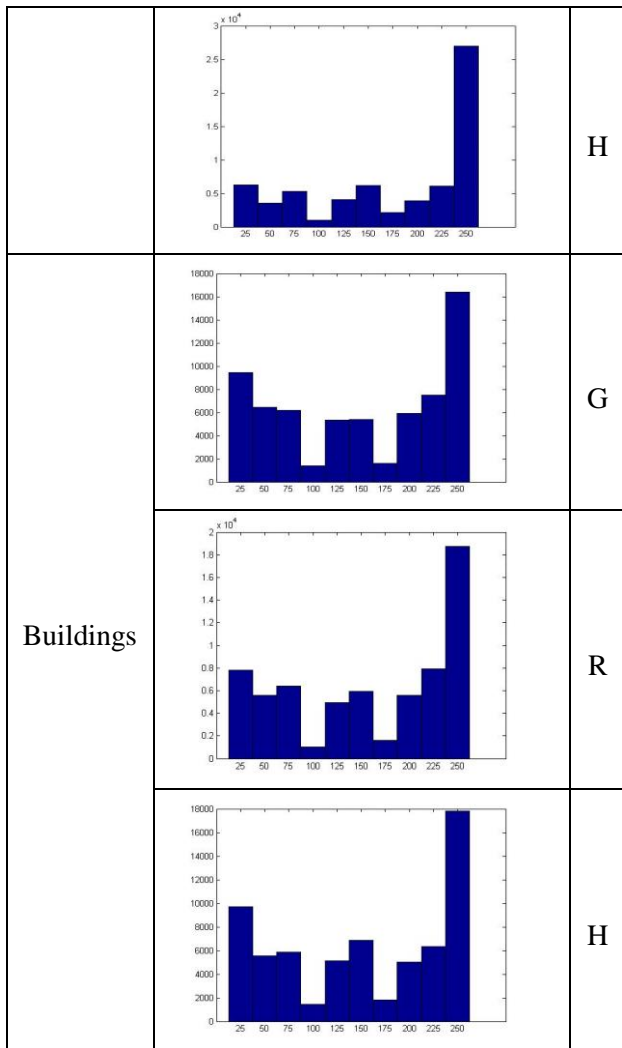
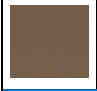
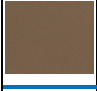
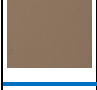
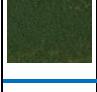
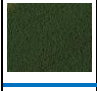






Fig.4. Average Histograms on color components.

Table 1 presents the results of the proposed algorithm in which the distances between the histogram vector of the tested sub-image and the average histogram vectors of the defined classes are shown. For example, the sub-image I\_4359\_f is affiliated to class flood since in all three color components the distances to this class are the lowest. There is also the case of sub-image I\_4889\_g that is eligible for grass class on only two color components. Following the presented methodology, this sub-image was classified to grass class.

The presented algorithm for flooded area detection was tested on a number of 100 sub-images extracted from different images that contain flooded areas. Overall, 98 images from 100 were classified to the correct class.

Table 1. Experimental result for flooded area detection on candidate sub-images

Sub-image	Distance from			Comp. worked	Decision class
	flood	grass	buildings		
I_4359_f	5.8207	10.0208	19.9156	H	flood
	7.5123	31.6125	32.7961	R	
	1.3950	24.5241	23.0662	G	
I_4376_f	6.1120	9.7940	19.8399	H	flood
	1.4183	37.4980	38.8386	R	
	1.4504	26.9866	25.6167	G	
I_4892_f	1.4126	14.4291	24.3621	H	flood
	2.5179	36.3981	37.7267	R	
	2.7619	28.3397	26.9828	G	
I_4889_g	11.6877	4.0846	14.1730	H	grass
	31.5503	8.9262	8.9668	R	
	21.9457	5.5310	3.2848	G	
I_4897_g	8.5872	7.4750	17.5284	H	grass
	38.4907	3.3232	3.5998	R	
	26.2877	1.6829	3.6996	G	
I_4898_g	19.8382	4.2190	6.0332	H	grass
	40.8614	2.4192	3.5144	R	
	27.1572	1.6737	4.7424	G	
I_4897_b	19.2540	4.4704	6.6784	H	buildings
	36.3156	7.0242	5.2606	R	
	24.3722	5.3157	3.5487	G	
I_4898_b	24.0252	8.9002	2.6653	H	buildings
	37.3744	6.2223	3.4625	R	
	25.1618	4.5534	1.9745	G	
I_4899_b	21.7087	6.5512	4.3617	H	buildings
	36.6832	7.0613	4.5562	R	
	24.5414	5.5657	2.9176	G	

## 5 Conclusion

In this paper we present a simple and efficient method for aerial image classification based on LBP operator extended to Green and Red channels of RGB and H of HSV. The images are obtained by the over-flight of an UAV and are grouped in three categories. The classification algorithm takes into consideration different sub-images from acquired images and it compares the resulted histogram vector with the every histogram vector of the defined classes. The method of comparison based on Euclidian distance offers good results in this classification process.

### Acknowledgment

The work has been funded by the Sectoral Operational Programme Human Resources Development 2007-2013 of the Ministry of European Funds through the Financial Agreement POSDRU 187/1.5/S/155420 and partially by National Research Programme STAR, project 71/2013: Multisensory robotic system for aerial monitoring of critical infrastructure systems-MUROS.

### References:

- [1] S.-W. Lo, J.-H. Wu, Lin, F.-P., C.-H. Hsu, Cyber Surveillance for Flood Disasters, *Sensors*, Vol. 15, 2015, pp. 2369-2387.
- [2] D. Popescu, L. Ichim, T. Caramihale, Image Recognition in UAV Application Based on Texture Analysis, *19th International Conference on System Theory, Control and Computing*, 2015, pp. 753-758.
- [3] Q. Feng, J. Liu, J. Gong, Urban Flood Mapping Based on Unmanned Aerial Vehicle Remote Sensing and Random Forest Classifier—A Case of Yuyao, China, *Water*, Vol. 7, 2015, pp. 1437-1455.
- [4] F. Nazir, M.M. Riaz, A. Ghafoor, F. Arif, Flood Detection/Monitoring Using Adjustable Histogram Equalization Technique, *The Scientific World Journal*, Vol. 2014, 2014, pp. 1-7.
- [5] S.-W. Lo, J.-H. Wu, L.-C. Chen, C.-H. Tseng, F.-P. Lin, Flood Tracking in Severe Weather, *International Symposium on Computer, Consumer and Control (IS3C)*, 2015, pp. 27-30.
- [6] M. Pietikäinen, T. Ojala, Z. Xu, Rotation-Invariant Texture Classification Using Feature Distributions, *Pattern Recognition*, Vol. 33, 2000, pp. 43-52.
- [7] M. Pietikäinen, A. Hadid, G. Zhao, T. Ahonen, Computer Vision Using Local Binary Patterns, *Computational Imaging and Vision*, Springer Vol. 40, 2011.
- [8] M. Prakash, J.M. Kezia, Texture Segmentation by a New Variant of Local Binary Pattern, *Proceedings of the Second International Conference on Computer and Communication Technologies*, Springer Vol. 380 AICS, 2015, pp 385-392.
- [9] S.H. Bhandari, A.G. Yadrave, Local binary pattern approach for rotation invariant texture classification, *International Conference on Circuit, Power and Computing Technologies (ICCPCT)*, 2015, pp. 1-4.
- [10] Z. Guo, D. Zhang, L. Zhang, A Complete Modelling of Local Binary Pattern Operator for Texture Classification, *IEEE Transactions on Image Processing*, Vol. 19, 2010, pp. 1657-1663.
- [11] C. Zhu, C.-E. Bichot, L. Chen, Multi-scale Color Local Binary Patterns for Visual Object Classes Recognition, *20<sup>th</sup> International Conference on Pattern Recognition*, 2010, pp. 3065-3068.
- [12] T. Ojala, M. Pietikainen, T. Maenpaa, Multiresolution Gray-Scale and Rotation Invariant Texture Classification with Local Binary Patterns, *IEEE Transactions on Pattern Analysis and Machine Intelligence*, Vol. 24, 2002, pp. 971-990.
- [13] W. Pratt, *Digital Image Processing*, PIKS Inside, Third Edition, John Wiley & Sons, Inc. 2001.
- [14] <http://www.teamnet.ro>.